Open forum

THE NUMERICAL THERMODYNAMIC ANALYSIS OF OTTO-MILLER CYCLE

by

Mehmet CAKIR

Department of Marine Engineering Operations, Yildiz Technical University, Istanbul, Turkey

Original scientific paper
DOI: 10.2298/TSCI150623131C

This paper presents a thermodynamic analysis for an irreversible Otto-Miller cycle by taking into consideration heat transfer effects and internal irreversibility resulting from compression and expansion processes. In the analyses, the influences of the Miller cycle ratio, combustion, and heat loss constants, and inlet temperature have been investigated relation with efficiency in dimensionless form. The dimensionless power output and power density and thermal efficiency relations have been computationally obtained vs. the engine design parameters with respect to combustion and heat transfer constants. The results demonstrate that the heat transfer and combustion constants have considerable effects on the cycle thermodynamic performance.

Key words: *Otto-Miller cycle, thermodynamic optimization, thermal efficiency*

Introduction

Internal combustion engines are commonly used in the daily life. Air-standard power cycle models are employed by most of the researchers to investigate numerical thermodynamic analysis of the internal combustion engines. Mozurkewich and Berry [1] studied the influences of the internal losses during the cycle processes of an Otto cycle and Hoffman *et al*. [2] conducted a similar study for diesel cycle. Miller cycle is a strategy of shortening compression stroke relative to expansion stroke. Miller cycle is more effective than Otto cycle and the heat transfer effects, friction and specific heat ratio on fuel efficiency are significant and must be observed in theoretical cycle analysis [3-8]. Wu *et al*. [9] analysed performance and optimization of a supercharged Otto-Miller cycle (OMC) engine. Klein [10] investigated a performance analysis for the purpose of investigate of the heat transfer effects through the engine walls of cylinder liner on the work for Otto and Diesel cycles. Analogously, Lin *et al.* [11] studied the performance of irreversible air standard Miller cycle in a four-stroke free-piston engine using finite-time thermodynamic. Sahin *et al*. [12] optimized an air-standard dual cycle by virtue of the ecological objective function. They studied the optimum performance and design parameters at maximum ecological performance criterion. Chen *et al*. [13] performed a study in order to investigate the power output and thermal efficiency relations for an air standard reversible Otto cycle considering the heat transfer loss from the cylinder wall. Angulo-Brown *et al.* [14] have presented an irreversible model for the air-standard Otto cycle, considering the finite times for

Authors' e-mail: mecakir@yildiz.edu.tr

heat added and heat loss processes. They climaxed the power output, thermal efficiency and ecological functions related to the compression ratio and demonstrated that the optimum compression ratio values for practical Otto engines. Ust *et al*. [15] proposed an irreversible model for on Otto heat engine and reported using thermodynamic analysis based on the maximum mean effective pressure, power, and thermal efficiency. Gonca *et al*. [16] studied the power output and thermal efficiency analysis for an air-standard irreversible Dual-Miller cycle.

In this study, a thermodynamic performance analysis implemented for an irreversible OMC based on the investigation of power output, power density, and thermal efficiency taking into the internal irreversibility arising from the compression and expansion processes. Furthermore, the various engine design parameters effects such as compression ratio, Miller cycle ratio, inlet temperatures on the performance of OMC have been analysed.

The thermodynamic analysis of the irreversible OMC

Figure 1 demonstrates *P-V* and *T-s* diagrams of the irreversible air-standard OMC. While s stands for isentropic processes which does not take into consideration the internal irreversibilities, the real heat input and output processes are 2-3 and 4-5, respectively, at constant volume and 5-1 at constant pressure.

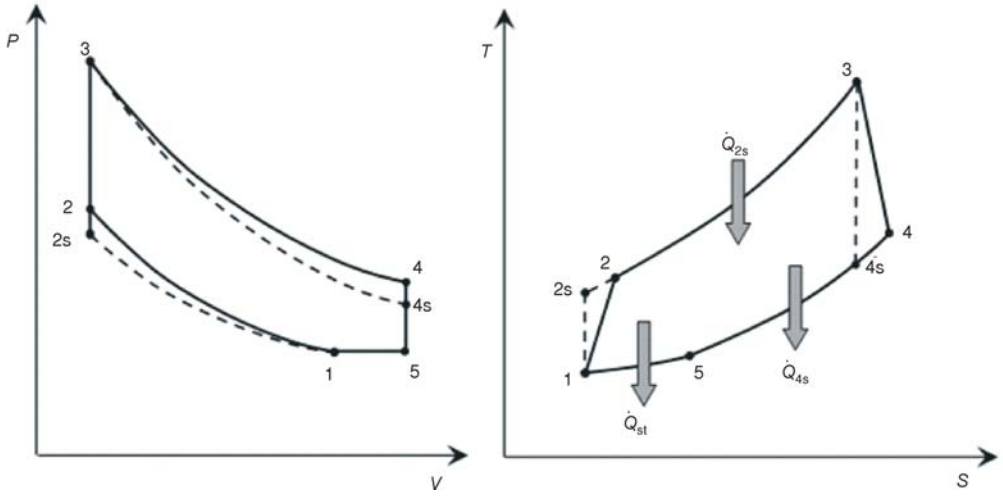

Figure 1. The *P-V* and *T-s* diagrams for the irreversible OMC

The total heat input and output are:

$$\dot{Q}_{\text{in}} = \dot{Q}_{23} = \dot{m}C_V (T_3 - T_2) \tag{1}$$

$$\dot{Q}_{\text{out}} = \dot{Q}_{45} + \dot{Q}_{51} = \dot{m}C_V (T_4 - T_5) + \dot{m}C_P (T_5 - T_1) \tag{2}$$

where T_1, T_2, T_3, T_4, and T_5 are temperatures at irreversible OMC, $\dot{m}$ is the mass flow rate C_V and C_P are the specific heat capacities of the ideal air. The power output according to the first law thermodynamics can be referred:

$$\dot{W} = \dot{Q}_{\text{in}} - \dot{Q}_{\text{out}} = \dot{m}C_V [(T_3 - T_2) - (T_4 - T_5) - k(T_5 - T_1)] \tag{3}$$

and the thermal efficiency is:

$$\eta = \frac{\dot{W}}{\dot{Q}_{\text{in}}} = 1 - \frac{\dot{Q}_{\text{out}}}{\dot{Q}_{\text{in}}} = 1 - \frac{T_4 - T_5 + k(T_5 - T_1)}{T_3 - T_2} \tag{4}$$

The dimensionless power output and power density of the cycle could be:

$$\overline{\dot{W}} = \frac{\dot{W}}{\dot{m}C_V T_1} = \frac{\dot{Q}_{\text{in}} - \dot{Q}_{\text{out}}}{\dot{m}C_V T_1} = \frac{\dot{m}C_V[(T_3 - T_2) - (T_4 - T_5) - k(T_5 - T_1)]}{\dot{m}C_V T_1} \tag{5}$$

$$\overline{\dot{W}}_{\text{d}} = \frac{\overline{\dot{W}}}{r_{\text{M}}} = \frac{(T_3 - T_2) - (T_4 - T_5) - k(T_5 - T_1)}{T_1 r_{\text{M}}} \tag{6}$$

In this part, Miller cycle ratio, r_{M} [17] is used to define the difference between OMC and Otto cycle. We can define the compression ratio (r), Miller ratio (r_{M}), stroke ratio (ε), pressure ratio (β), and cycle temperature ratio (α) [16]:

$$r = \frac{v_1}{v_2} \tag{7}$$

$$r_{\text{M}} = \frac{v_5}{v_1} = \frac{T_5}{T_1} \tag{8}$$

$$\varepsilon = r_{\text{M}} r = \frac{v_5}{v_2} \tag{9}$$

OMC equals to Otto cycle if $r_{\text{M}} = 1$.

$$\beta = \frac{P_3}{P_2} = \frac{T_3}{T_2} \tag{10}$$

$$\alpha = \frac{T_{\max}}{T_{\min}} = \frac{T_3}{T_1} \tag{11}$$

The second law of thermodynamics requires that $s_{2s3} = s_{4s5} + s_{51}$ and the result is:

$$T_{2s} T_{4s} T_5^{k-1} = T_3 T_1^k \tag{12}$$

Isentropic efficiency of the compression and expansion processes (1-2 and 3-4) are written [18]:

$$\eta_{\text{C}} = \frac{T_{2s} - T_1}{T_2 - T_1} \tag{13}$$

and

$$\eta_{\text{E}} = \frac{T_3 - T_4}{T_3 - T_{4s}} \tag{14}$$

By using eqs. (13) and (14) and re-ordering the design parameters of the OMC, the temperatures of the state 2 and 4 are written:

$$T_2 = T_1 \left[1 + \frac{r^{k-1} - 1}{\eta_{\text{C}}} \right] \tag{15}$$

and

$$T_4 = T_3 \left[1 - \eta_{\text{E}} \left(1 - \frac{1}{\varepsilon^{k-1}} \right) \right] \tag{16}$$

Klein [10] asserted that the heat input to the working fluid at the constant volume processes could be:

$$\dot{Q}_{23} = a - b(T_2 + T_3) \tag{17}$$

where a and b are the heat release (combustion) and heat loss constants during the combustion processes, respectively. The T_3 can be re-written by using these constants:

$$T_3 = \frac{a + (C_V - b)T_1\left(1 + \dfrac{r^{k-1} - 1}{\eta_C}\right)}{C_V + b} \tag{18}$$

If we intraduce eq. (18) into eq. (16), one can obtain:

$$T_4 = \frac{a + (C_V - b)T_1\left(1 + \dfrac{r^{k-1} - 1}{\eta_C}\right)}{C_V + b}\left[1 - \eta_\varepsilon\left(1 - \frac{1}{\varepsilon^{k-1}}\right)\right] \tag{19}$$

The relationship between T_1 and T_5 is:

$$T_5 = T_1 r_M \tag{20}$$

The dimensionless power output, power density, and thermal efficiency of the cycle can be expressed by substituting eqs. (15), (18), (19), and (20) into eqs. (4), (5), and (6):

$$\overline{\dot{W}} = \alpha\eta_E\left(1 - \frac{1}{\varepsilon^{k-1}}\right) - \left(1 + \frac{r^{k-1} - 1}{\eta_C}\right) + r_M(1 - k) + k \tag{21}$$

$$\overline{\dot{W}}_d = \frac{\alpha\eta_E}{r_M}\left(1 - \frac{1}{\varepsilon^{k-1}}\right) - \left(\frac{1}{r_M} + \frac{r^{k-1} - 1}{r_M\eta_C}\right) - k\left(1 - \frac{1}{r_M}\right) + 1 \tag{22}$$

$$\eta = 1 - \frac{\dot{Q}_{out}}{\dot{Q}_{in}} = \frac{\alpha\eta_E\left(1 - \dfrac{1}{\varepsilon^{k-1}}\right) - \left(1 + \dfrac{r^{k-1} - 1}{\eta_C}\right) + r_M(1 - k) + k}{\alpha - \left(1 + \dfrac{r^{k-1} - 1}{\eta_C}\right)} \tag{23}$$

All equations have been written in engineering equation solver [19] and numerical solutions and comparative figures have been obtained.

Results and discussion

The following parameters have been used in this analysis: $k = 1.4$, $C_V = 0.718$ kJ/kgK, $a = 2500$-3500 kJ/kg, $b = 0.4$-0.7 kJ/kgK, $r_M = 1$-4, $T_1 = 300$-400 K, $\eta_C = 0.85$, and $\eta_\varepsilon = 0.90$ [5, 13, 20]. Using these constants and parameters, dimensionless power output and density *vs*. thermal efficiency and compression ratio *vs*. thermal efficiency could be plotted in figs. 2-7.

The figs. 2 and 3 demonstrates the influence of a and b constants on the dimensionless power output, power density, and thermal efficiency ($\overline{\dot{W}}$, $\overline{\dot{W}}_d$ and η) Black, blue, and red lines (for color lines see journal web site) on the graph refers dimensionless power output for $r_M = 1$ (Otto cycle), dimensionless power output for $r_M = 2$, and dimensionless power density for $r_M = 2$, respectively. In fig. 2, the dimensionless power output and density *vs.* thermal efficiency increase with increasing of the a parameter. Increasing a causes an increase at the amount of heat added to the working fluid due to combustion. Also, the thermal efficiency performance increases with in-

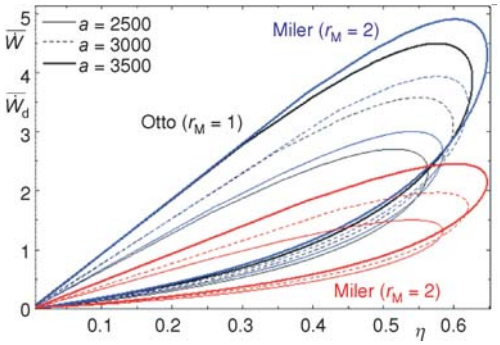

Figure 2. $\overline{W}$, $\overline{W}_d$ from η in function of different *a* combustion constant for the irreversible OMC (T_1 = 300 K, *b* = 0.4 kJ/kgK)

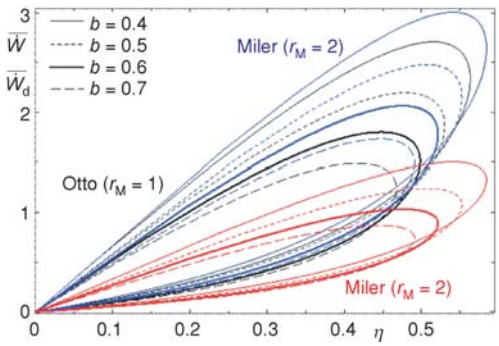

Figure 3. $\overline{W}$, $\overline{W}_d$ from η in function of different *b* heat transfer coefficients for the irreversible OMC (T_1 = 300 K, *a* = 2500 kJ/kgK)

creasing r_M and this situation holds for variation of *b* constant in fig. 3. While the dimensionless power output and power density *vs*. thermal efficiency increase with rise of *a* constant, they decrease with rise of *b* constant. This situation is similar to that of previous studies [11, 20, 21].

The influence T_1 on the performance is shown in fig. 4. Volumetric efficiency of cycle reduces with increasing T_1. So, the mass of working fluid reduces for cycle. Hence, the performance decreases in all conditions with increasing T_1. Hou [5] also obtained similar results about the effect T_1 on the performance of the dual cycle.

The dimensionless power output, power density, and thermal efficiency relation is shown with variation of different r_M in fig. 5. The loop curves of dimensionless power output, power density, and thermal efficiency become bigger up to r_M = 2 and then begin to decline when r_M increases. According to these curves, the ideal Miller ratio is r_M = 2 value. In fig. 6, the dimensionless power output, power density, and compression ration relation is shown with variation of different r_M. Here, maximum dimensionless power outputs approximately are r = 10 value for all of r_M values. This situation holds for dimensionless power density. The maximum dimensionless power output is similar for Miller ratio 1.5 and 2. After this point, if Miller ratio increases, the dimensionless power output decreases. The dimensionless power density is maxi-

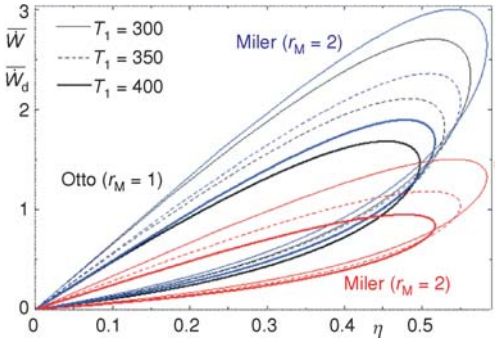

Figure 4. $\overline{W}$, $\overline{W}_d$ from η in function of different T_1 temperatures for the irreversible OMC (*a* = 2500 kJ/kg, *b* = 0.4 kJ/kgK)

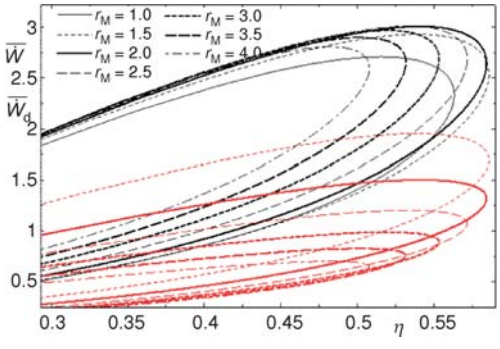

Figure 5. $\overline{W}$, $\overline{W}_d$ from η in function of different r_M for the irreversible OMC (T_1 = 300 K, *a* = 2500 kJ/kg, *b* = 0.4 kJ/kgK)

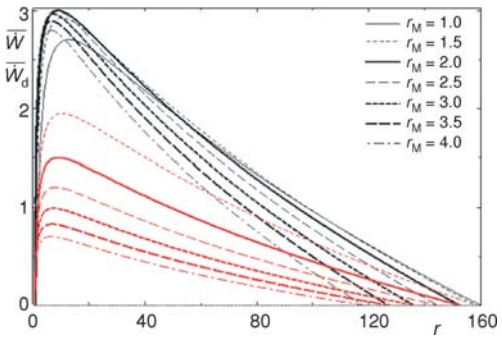

Figure 6. $\bar{W}$, $\bar{W}_d$ from η in function of different r_M for the irreversible OMC (T_1 = 300 K, a = 2500 kJ/kg, b = 0.4 kJ/kgK)

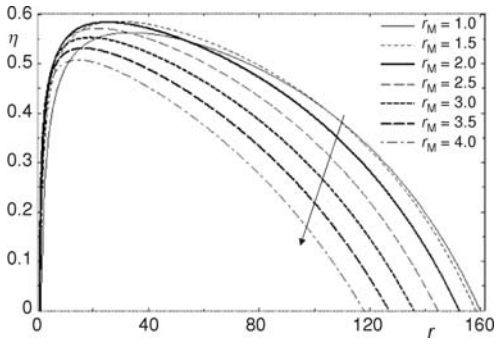

Figure 7. η-r relation with variation of different r_M for the irreversible OMC (T_1 = 300 K, a = 2500 kJ/kg, b = 0.4 kJ/kgK)

mum for r_M = 1.5. After this point, the higher Miller ratio, the dimensionless power density gradually decreases.

The thermal efficiency and compression ratio relation is shown with variation of different r_M in fig. 7. Here, the maximum thermal efficiencies corresponding compression ratios could be observed for various r_M values. As it can be seen, the cycle thermodynamic performance increases to a certain value and then begins to reduce with increasing compression ratio. It could be observed that maximum thermal efficiency and corresponding compression ratio is similar for r_M = 1.5 and r_M = 2. But, as fig. 5 can be observed, idealist loop curve of dimensionless power out is r_M = 2 value.

Conclusions

This paper analyses the optimum cycle thermodynamic performance. The obtained results can be used to determine engine design parameters. Therefore, it is analysed the influences different Miller cycle ratio (r_M), inlet temperature (T_1), combustion and heat loss constants (a, b) on the dimensionless power output, power density, and thermal efficiency. By considering the internal irreversibilities and heat transfer influences, the relevance between the dimensionless power output and power density with respect to thermal efficiency have been shown. The results prove that the combustion and heat transfer constants have considerable effects on the cycle thermodynamic performance. This situation theoretically is demonstrated for OMC. The theoretical Otto cycle thermodynamic performance rises with increase in the Miller cycle ratio and combustion constant (a) with the reduction in the inlet temperature and heat transfer constant (b). Consequently, optimum Miller ratio attempted to be determining for irreversible OMC. Using these graphs, the future studies can be investigated in combustion engine conditions for OMC.

Nomenclature

a – combustion constant at constant volume process, [kJkg^{-1}]
b – heat transfer constant at constant volume process, [kJkg^{-1}K^{-1}]
C_p – specific heat at constant pressure, [kJkg^{-1}K^{-1}]
C_V – specific heat at constant volume, [kJkg^{-1}K^{-1}]
k – isentropic exponent
r – compression ratio
r_M – Miller cycle ratio
P – pressure, [kPa]
$\dot{Q}$ – heat rate, [kW]
s – entropy, [kJK^{-1}]
T – temperature, [K]
V – volume, [m^3]

v – specific volume, [m^3kg^{-1}]
W – power output, [kW]
$\dot{W}_d$ – power density

Greek symbols

α – cycle temperature ratio
β – pressure ratio, (= T3/T2)
ε – stroke ratio
h – thermal efficiency
η_C – compression efficiency
η_E – expansion efficiency

Superscripts

. – time-dependent condition
– – non-dimensional

References

[1] Mozurkewich, M., Berry, R. S., Optimal Paths for Thermodynamic Systems: The Ideal Otto Cycle, *J Appl Phys., 53* (1982), 1, pp. 34-42
[2] Hoffman, K. H., *et al*., Optimal Paths for Thermodynamic Systems: The Ideal Diesel Cycle, *J Appl Phys, 58* (1985), 6, pp. 2125-2134
[3] Ge, Y., *et al*., Thermodynamic Simulation of Performance of an Otto Cycle with Heat Transfer and Variable Specific Heats for the Working Fluid, *Int. J. Therm. Sci., 44* (2005), 5, pp. 506-511
[4] Ge, Y., *et al*., Finite-Time Thermodynamic Modelling and Analysis of an Irreversible Otto-Cycle, *Appl. Energy, 85* (2007), 7, pp. 618-624
[5] Hou, S. S., Heat Transfer Effects on the Performance of an Air Standard Dual Cycle, *Energy Convers. Mgmt, 45* (2004), 18-19, pp. 3003-3015
[6] Ozsoysal, O. A., Heat Loss as a Percentage of the Fuel's Energy in Air-standard Otto and Diesel Cycles, *Energy Convers. Mgmt, 47* (2006), 7-8, pp. 1051-1062
[7] Al-Sarkhi, A., *et al*., Efficiency of a Miller Engine, *Appl Energ, 83* (2006), 4, pp. 343-351
[8] Li, T., *et al.*, The Miller Cycle Effects on Improvement of Fuel Economy in a Highly Boosted, High Compression Ratio, Direct-Injection Gasoline Engine: EIVC *vs*. LIVC, *Energy Conversion and Management, 79* (2014), Mar., pp. 59-65
[9] Wu, C., *et al.*, Performance Analysis and Optimization of a Supercharged Miller Cycle Otto Engine, *Appl. Therm. Eng., 23* (2003), 5, pp. 511-521
[10] Klein, S. A., An Explanation for Observed Compression Ratios in Internal-Combustion Engines, *Trans ASME J. Eng. Gas Turb Pow., 113* (1991), 4, pp. 511-513
[11] Lin, J., *et al*., Finite-Time Thermodynamic Modeling and Analysis of an Irreversible Miller Cycle Working on a Four-Stroke Engine, *Int. Communications in Heat and Mass Transfer, 54* (2014), May, pp. 54-59
[12] Sahin, B., *et al*., A Comparative Performance Analysis of Endoreversible Dual-Cycle under Maximum Ecological Function and Maximum Power Conditions, *Exergy, Int. J, 2* (2002), 3, pp. 173-185
[13] Chen, L., *et al*., Heat-Transfer Effects on the Net Work-Output and Efficiency Characteristics for an Air Standard Otto Cycle, *Energy Convers. Mgmt, 39* (1998), 7, pp. 643-648
[14] Angulo-Brown, F., *et al*., A Non-Endoreversible Otto Cycle Model: Improving Power Output and Efficiency, *J Phys:D Appl Phys, 29* (1996), 1, pp. 80-83
[15] Ust, Y., *et al*., The Effects of Cycle Temperature and Cycle Pressure Ratios on the Performance of an Irreversible Otto Cycle, *Acta Physica Polonica A, 120* (2011), 3, pp. 412-416
[16] Gonca, G., *et al*., Performance Maps for an Air-Standard Irreversible DMC with LIVC Version, *Energy, 54* (2013), Jun., pp. 285-290
[17] Wang, Y., *et al*., An Analytic Study of Applying Miller Cycle to Reduce NO_x Emission from Petrol Engine, *Appl Therm Eng., 27* (2007), 11-12, pp. 1779-1789
[18] Ge, Y., *et al*., Finite-Time Thermodynamic Modeling and Analysis for an Irreversible Dual Cycle, *Mathematical and Computer Modelling, 50* (2009), 1-2, pp. 101-108
[19] ***, EES Academic Professional Edition V.9.170-3D, USA, F-Chart Software, 2012
[20] Ust, Y., *et al*., Heat Transfer Effects on the Performance of an Air-Standard Irreversible Otto Cycle, 11th Int. Combust. Symp., Sarajevo, Bosnia and Herzegovina, 2010
[21] Ust, Y., *et al*., Heat Transfer Effects on the Performance of an Air-Standard Irreversible Dual Cycle, *Int. J. Vehicle Design, 63* (2013), 1, pp. 102-116

Paper submitted: June 23, 2015
Paper revised: August 11, 2015
Paper accepted: August 12, 2015